JOURNAL OF BACTERIOLOGY, Dec. 2007, p. 9001–9010 Vol. 189, No. 24
0021-9193/07/$08.00+0 doi:10.1128/JB.01172-07

The Division Inhibitor EzrA Contains a Seven-Residue Patch Required for Maintaining the Dynamic Nature of the Medial FtsZ Ring[▽]

Daniel P. Haeusser, Anna Cristina Garza, Amy Z. Buscher, and Petra Anne Levin*

Department of Biology, Washington University, St. Louis, Missouri 63130

Received 24 July 2007/Accepted 4 September 2007

The essential cytoskeletal protein FtsZ assembles into a ring-like structure at the nascent division site and serves as a scaffold for the assembly of the prokaryotic division machinery. We previously characterized EzrA as an inhibitor of FtsZ assembly in *Bacillus subtilis*. EzrA interacts directly with FtsZ to prevent aberrant FtsZ assembly and cytokinesis at cell poles. EzrA also concentrates at the cytokinetic ring in an FtsZ-dependent manner, although its precise role at this position is not known. Here, we identified a conserved patch of amino acids in the EzrA C terminus that is essential for localization to the FtsZ ring. Mutations in this patch (designated the "QNR patch") abolish EzrA localization to midcell but do not significantly affect EzrA's ability to inhibit FtsZ assembly at cell poles. *ezrA* QNR patch mutant cells exhibit stabilized FtsZ assembly at midcell and are significantly longer than wild-type cells, despite lacking extra FtsZ rings. These results indicate that EzrA has two distinct activities in vivo: (i) preventing aberrant FtsZ ring formation at cell poles through inhibition of de novo FtsZ assembly and (ii) maintaining proper FtsZ assembly dynamics within the medial FtsZ ring, thereby rendering it sensitive to the factors responsible for coordinating cell growth and cell division.

At the onset of cell division, the tubulin-like FtsZ protein assembles into a membrane-associated ring that establishes the division site in most bacteria and archaea, as well as in chloroplasts and the mitochondria of certain protists (21). The FtsZ ring is present for a large portion of the cell cycle (the Z-period), serving as a scaffold for assembly of the division apparatus and constricting at the leading edge of the invaginating septum at the onset of division (10).

Like tubulin, FtsZ assembly dynamics result from GTP binding and hydrolysis. In vitro GTP binding induces FtsZ assembly into single-stranded polymers. These polymers then interact laterally to form the bundles (19, 23) that are thought to constitute the FtsZ ring in vivo (21, 25). Subsequent GTP hydrolysis destabilizes FtsZ polymers, which become curved and rapidly disassemble (25).

In the cell, FtsZ exists in a precise balance between the membrane-associated single-stranded polymers and bundles that constitute the FtsZ ring and the cytoplasmic monomers and small multimers that constitute the pool of FtsZ subunits available for exchange into the cytokinetic ring (21, 25). Disturbances in FtsZ assembly dynamics result in aberrant division events or potentially lethal filamentation (10, 21, 25). The FtsZ ring itself is a highly dynamic structure. Fluorescence recovery after photobleaching (FRAP) experiments have indicated that the half-life of an individual subunit is between 4 and 20 s (1). Maintaining the precise balance between FtsZ assembly and disassembly is critical for coordinating division with cell growth and to ensure that daughter cells each receive a full genetic complement following cytokinesis (10, 21, 25).

FtsZ levels are constant throughout the cell cycle, and the spatial and temporal control of division is governed primarily at the level of FtsZ assembly (30). To date, a few proteins that modulate FtsZ assembly dynamics in vivo have been identified (6, 10). One of these proteins, EzrA, is an inhibitor that prevents aberrant FtsZ assembly at the poles of exponentially growing cells (8, 17, 19).

EzrA is found throughout the low-G+C-content gram-positive bacteria and exhibits significant structural conservation. EzrA is anchored in the plasma membrane by an N-terminal transmembrane domain. The remainder of the EzrA polypeptide consists of a series of predicted cytoplasmic coiled-coil domains (17). This somewhat unusual topology (N terminus out topology) is shared with ZipA, a cell division protein that is found in the gamma subdivision of the *Proteobacteria* (9). Null mutations in *ezrA* lower the concentration of FtsZ required for assembly in vivo, leading to the formation of polar FtsZ rings and septa (17) and stabilizing FtsZ assembly at midcell (19).

A purified thioredoxin-EzrA fusion lacking the EzrA transmembrane anchor (Thio-EzrA) interacts with FtsZ in vitro and inhibits FtsZ assembly in both sedimentation and 90°-angle light-scattering assays (8). Deletion analysis has indicated that EzrA interacts with the C-terminal 16 residues of FtsZ to inhibit assembly in vitro (28). It has recently been reported that addition of the native cytoplasmic portion of EzrA results in a modest (1.6-fold) increase in FtsZ GTP hydrolysis (5), suggesting that EzrA may increase subunit turnover. However, the precise mechanism by which EzrA modulates FtsZ ring formation remains unknown, as an EzrA fusion protein lacking the transmembrane domain

* Corresponding author. Mailing address: Department of Biology, Washington University, St. Louis, MO 63130. Phone: (314) 935-7888. Fax: (314) 935-4432. E-mail: plevin@biology.wustl.edu.

▽ Published ahead of print on 14 September 2007.

TABLE 1. Strains used

Strain	Genotype	Reference or source
JH642	*B. subtilis trpC2 pheA1*	24
PL847	JH642 *ezrA*::*ezrA-gfp spc*	17
PL872	JH642 *ezrA*::*ezrA*Δ*377-562-gfp spc*	This study
PL1626	JH642 *ezrA*::*ezrA*Δ*436-562-gfp spc*	This study
PL1628	JH642 *ezrA*::*ezrA*Δ*500-562-gfp spc*	This study
PL1630	JH642 *ezrA*::*ezrA*Δ*551-562-gfp spc*	This study
PL1693	JH642 *ezrA*::*ezrA*Δ*501-511-gfp spc*	This study
PL1718	JH642 *ezrA*::*ezrA*(*Q506A*)*-gfp spc*	This study
PL1719	JH642 *ezrA*::*ezrA*(*N509A*)*-gfp spc*	This study
PL1776	JH642 *ezrA*::*ezrA*(*R510D*)*-gfp spc*	This study
PL1900	JH642 *ezrA*::*ezrA*(*R510A*)*-gfp spc*	This study
PL867	JH642 *ezrA*::*spc*	17
PL1737	JH642 *ezrA*::*ezrA*(*Q506A*) *spc*	This study
PL1739	JH642 *ezrA*::*ezrA*(*N509A*) *spc*	This study
PL1780	JH642 *ezrA*::*ezrA*(*R510D*) *spc*	This study
PL1940	JH642 *ezrA*::*ezrA*(*R510A*) *spc*	This study
PL1145	JH642 *thrC*::P_{spachy}*-minCD erm*	31
MO45	JH642 *ezrA*::*kan*	This study
MO49	JH642 *thrC*::P_{spachy}*-minCD erm ezrA*::*kan*	This study
PL1749	JH642 *thrC*::P_{spachy}*-minCD erm ezrA*::*ezrA*(*Q506A*) *spc*	This study
PL1750	JH642 *thrC*::P_{spachy}*-minCD erm ezrA*::*ezrA*(*N509A*) *spc*	This study
PL1787	JH642 *thrC*::P_{spachy}*-minCD erm ezrA*::*ezrA*(*R510D*) *spc*	This study
PL1963	JH642 *thrC*::P_{spachy}*-minCD erm ezrA*::*ezrA*(*R510A*) *spc*	This study
PL642	JH642 *ftsZ*::*ftsZ-gfp cat*	17
PL876	JH642 *ftsZ*::*ftsZ-gfp cat ezrA*::*spc*	This study
PL1752	JH642 *ftsZ*::*ftsZ-gfp cat ezrA*::*ezrA*(*Q506A*) *spc*	This study
PL1753	JH642 *ftsZ*::*ftsZ-gfp cat ezrA*::*ezrA*(*N509A*) *spc*	This study
PL1827	JH642 *ftsZ*::*ftsZ-gfp cat ezrA*::*ezrA*(*R510D*) *spc*	This study
PL1971	JH642 *ftsZ*::*ftsZ-gfp cat ezrA*::*ezrA*(*R510A*) *spc*	This study
AG1111	DZR200 [= MC1061 F′ *lacI*^{q} *lacZM15* Tn*10*(Tet)]	12
ER2566	F$^-$ λ$^-$ *fhuA2* [*lon*] *ompT lacZ*::*T7 gene 1 gal sulA11* Δ(*mcrC-mrr*)*114*::IS*10* *R*(*mcr-73*::mini-Tn*10*(Tet^s)*2 R*(*zgb-210*::Tn*10*)(Tet^s) *endA1*[*dcm*]	Lab stock
PL1184	ER2566/pBS58/pCXZ	8
BB101	*slyD lac pro* F′ (*lacI*^{q}) *ara lac pro nalA argE*(Am) (λDE3)	3
PL1364	BB101 P_{BAD} Thio-EzrAΔTM-His_6 TOPO	8
PL1821	BB101 P_{BAD} Thio-EzrAΔTM(R510D)-His_6 TOPO	This study

effectively inhibits FtsZ assembly in vitro without altering FtsZ's intrinsic GTPase activity (8).

EzrA exhibits two distinct patterns of subcellular localization. In predivisional cells EzrA is uniformly distributed throughout the plasma membrane. Paradoxically, given its ability to inhibit FtsZ assembly, EzrA also concentrates at the division site in an FtsZ-dependent manner (17). EzrA's role at midcell is unclear. EzrA localization to the medial ring may simply be a consequence of residual interaction with FtsZ. Alternatively, EzrA may promote subunit turnover at midcell. Arguing against the latter model, FRAP experiments on FtsZ rings have indicated that there is little change in subunit turnover in the absence of EzrA (1). However, cells lacking EzrA are significantly longer than wild-type cells (4, 14, 17), consistent with altered FtsZ assembly dynamics at midcell that disrupt the coupling of division with cell growth.

To clarify the role of EzrA at midcell, we employed a combination of deletion analysis and site-directed mutagenesis to identify regions of EzrA that are required for medial localization. Using this approach, we identified a conserved seven-residue patch (designated the "QNR patch" after the three most conserved residues) that is required for EzrA localization to the FtsZ ring. A single substitution in the QNR patch abolishes medial EzrA localization, but it does not alter the ability of EzrA to inhibit FtsZ assembly in vitro and results in only a negligible increase in polar FtsZ assembly. However, despite lacking extra FtsZ rings, *ezrA* QNR patch mutant cells are longer than their wild-type counterparts and exhibit stabilized FtsZ assembly at midcell, similar to *ezrA* null mutant cells. Together, our results support a model in which EzrA has two distinct functions in vivo: (i) preventing aberrant FtsZ ring formation by inhibiting de novo FtsZ assembly at cell poles and (ii) maintaining proper FtsZ assembly dynamics within the medial FtsZ ring.

MATERIALS AND METHODS

General methods and strain construction. Strains are listed in Table 1. All *Bacillus subtilis* strains are derivatives of JH642 (24). Cloning and genetic manipulation were performed using standard techniques (11, 26). *Escherichia coli* strain AG1111 (12) was used for plasmid construction, unless otherwise noted. Vent DNA polymerase (NEB) and Klen*taq*LA (DNA Polymerase Technology, Inc.) were used for PCRs. All oligonucleotide sequences and plasmid information are available upon request.

Luria-Bertani (LB) medium was used unless otherwise noted, and cells were grown at 37°C (strains bearing the wild-type *ftsZ* allele) or at 30°C [strains bearing the heat-sensitive *ftsZ*(Ts) (*ftsZ-gfp*) allele]. Chloramphenicol (Sigma) was used at a final concentration of 5 μg/ml, spectinomycin (Sigma) was used at a final concentration of 100 μg/ml, kanamycin (EM Sciences) was used at a final concentration of 10 μg/ml, and ampicillin (Fisher Scientific) was used at a final concentration of 100 μg/ml. Strains resistant to macrolides, lincosamides, and

streptogramins were cultured in media containing erythromycin (Fisher Scientific) at a final concentration of 0.5 μg/ml and lincomycin (ICM Biomedicals) at a final concentration of 2.5 μg/ml. Isopropyl-β-D-thiogalactopyranoside (IPTG) (Sigma) was used at a concentration of 1 mM.

The *ezrA*::*kan* null mutation was created by inserting a 1.4-kb kanamycin cassette between codons 147 and 285 of *ezrA*. The *kan* cassette was removed from pGK67 (15) by SmaI/PstI (NEB) digestion and ligated into a 1.1-kb *ezrA* fragment within a derivative of pCR2.1 (Invitrogen) digested with PstI/Eco47III (NEB). The resulting plasmid was transformed into JH642 for *ezrA*::*kan* integration at the native *ezrA* locus by double-crossover homologous recombination with selection for kanamycin resistance. Proper integration was verified by PCR.

C-terminal EzrA truncations that were fused to green fluorescent protein (GFP) were created in pPL65 (a derivative of pUS19 [2] containing a ~900-bp 3′ *ezrA* fragment fused to *gfp*). The wild-type *ezrA* fragment was cut from the vector by EcoRI/XhoI (NEB) digestion and replaced with a relevant *ezrA* truncation fragment amplified by PCR from the JH642 chromosome. All *ezrA-gfp* point mutations and the *ezrAΔ501-511-gfp* deletion were created using a QuikChange site-directed mutagenesis kit (Stratagene) on pPL65. Tagless mutants lacking GFP were constructed by PCR amplifying the *ezrA* fragment (residues 355 to 562) with EcoRI/BamHI (NEB) linkers from the pPL65 derivatives and placing them into pUS19. The resulting plasmids were transformed into JH642 with selection for single-crossover recombination events at the native *ezrA* locus by growth on spectinomycin-containing media. Mutations were confirmed by plasmid sequencing, and integration was confirmed by chromosomal *ezrA* locus sequencing.

Strains used for the *minCD* and *ftsZ*(Ts) suppression assays were constructed by transforming the chromosome from the tagless *ezrA* mutant strains into the relevant background and selecting for the appropriate antibiotic resistance. *minCD* and *ftsZ*(Ts) suppression assays were conducted as previously described (19, 31).

The Thio-EzrAΔTM(R510D)-His_6 fusion [Thio-EzrA(R510D)] under P_{BAD} control (7) was constructed by amplification of full-length *ezrAΔTM*(*R510D*) from PL1780, followed by TOPO cloning (Invitrogen) as described previously for the wild-type EzrA fusion (Thio-EzrA) (8). After the mutation within the plasmid was verified by sequencing, the plasmid was transformed into "One Shot chemically competent" TOP10 cells (Invitrogen) and then isolated and transformed into a BB101 background (3) for protein induction and purification.

Microscopy. Fluorescence microscopy was performed as described previously (17). An Olympus BX51 microscope with Chroma filters and a Hamamatsu OrcaERG camera were used for image capture. Images were processed using Openlab version 5.0.1 (Improvision) and Adobe Photoshop CS version 8.0 (Adobe Systems). All cell or ring measurements for collected images were obtained with a minimum population of 200 cells/strain.

GFP fusions were visualized in live cells as described previously (16). Briefly, cells grown to mid-exponential phase (optical density at 600 nm, ~0.4) in liquid culture were stained with the vital membrane dye FM 4-64 (Invitrogen) at a dilution of 1:2,000 for 1 to 3 min and then placed on 1% agarose in 1× phosphate-buffered saline pads (16) on glass microscope slides. EzrA-GFP localization to midcell was scored as strong, weak, or none based on fluorescent band intensity. Statistical analysis of EzrA-GFP localization between strains was performed using a χ^2 test with 2 df and a significance level (α) of 0.001.

Cells were prepared for immunofluorescence microscopy by paraformaldehyde and glutaraldehyde treatment, as described previously (16, 17), with lysozyme incubation typically lasting 7 to 10 min. FtsZ was detected using affinity-purified polyclonal rabbit anti-FtsZ sera (18) in combination with donkey anti-rabbit sera conjugated to Cyanine-3 (Jackson Immunoresearch). Cell walls were visualized with wheat germ agglutinin conjugated to fluorescein (Invitrogen). Statistical analysis of FtsZ localization between strains was performed using a χ^2 test (5 df; $\alpha = 0.001$.

Cell lengths were measured with fixed cells, using a 3- to 4-min lysozyme treatment that better preserved cell wall structure. Septa were defined as bands of fluorescent signal that fully traversed the cell width with intensity equal to or greater than the intensity of lateral wall fluorescence. Cell length data were obtained with Openlab software and exported to Microsoft Excel (version 11.1) for analysis. Statistical analysis of cell lengths between strains was performed using a χ^2 test (5 df; $\alpha = 0.001$). Length-to-ring ratios were determined as described previously (29, 32).

Protein purification. *B. subtilis* FtsZ was purified from PL1184, an *E. coli* ER2566 derivative, as described previously (8, 31). Thio-EzrA and Thio-EzrA(R510D) were purified from *E. coli* BB101 (3) derivatives (PL1364 and PL1821, respectively) as described previously (8). A size exclusion chromatography step was added to our original protocol to remove EzrA degradation products that frequently caused aggregation and precipitation of the final product.

One-liter cultures of cells containing induced Thio-EzrA or Thio-EzrA(R510D) were pelleted, washed in EzrA induction buffer (50 mM $NaPO_4$ [pH 8.0], 300 mM NaCl), repelleted, and frozen at −80°C for later use. On the day of purification, cell pellets were thawed and resuspended in 30 ml of ice-cold EzrA induction buffer containing 1 mM 4-(2-aminoethyl)benzenesulfonyl fluoride hydrochloride (Sigma). Cells were lysed by two or three passes in a prechilled, 30-ml-capacity French press cell at 1,000 lb/in^2. All subsequent steps were performed at 4°C. Lysates were cleared by centrifugation as described previously (8) and loaded in EzrA buffer 350 (50 mM HEPES [pH 7.5], 350 mM NaCl) containing 50 mM imidazole onto two tandem 5-ml Hi-Trap chelating HP columns (GE Healthcare) charged with nickel on an ÄKTA prime low-pressure purification system (GE Healthcare). Bound EzrA was washed with EzrA buffer 350 containing 75 mM imidazole, and bound protein was eluted in one step with EzrA buffer 350 containing 200 mM imidazole. Peak fractions were pooled, concentrated to ~1 to 2 ml using Centricon YM-50 filters (Fisher Scientific), and applied to an S300 gel filtration column (GE Healthcare) preequilibrated with EzrA buffer 175 (50 mM HEPES [pH 7.5], 175 mM NaCl, 1 mM EGTA). Both the Thio-EzrA and Thio-EzrA(R510D) proteins eluted in three peaks: a small inactive aggregate peak, an active peak with the apparent molecular weight of a dimer, and an inactive peak with the apparent molecular weight of a monomer. Fractions from the active peak were collected, pooled, and concentrated with YM-50 filters. Glycerol was added to a final concentration of 10%, and aliquots were flash frozen at −80°C.

The FtsZ protein concentration was determined by using an average of bicinchoninic acid (Pierce) and Coomassie Plus (Pierce) assay estimates, while EzrA fusion concentrations were estimated by bicinchoninic acid and Coomassie Plus assays, as well as by using A_{280} (molar extinction coefficient, 58,656.0 A_{280}/mol as determined by Gene Inspector, version 1.6.3 [Textco]) and a SPECTRAmax Plus spectrophotometer (Molecular Devices).

90°-angle light-scattering assay. Light-scattering assays were conducted essentially as described previously (8, 31) using a DM-45 spectrofluorimeter (Olis). Readings were taken four times per second at 30°C, and a baseline was determined for 1 min before addition of 1 mM GTP to the cuvette. The reaction mixtures contained 5 μM FtsZ diluted in polymerization buffer [50 mM morpholineethanesulfonic acid (MES) (pH 6.5), 2.5 mM $Mg(CH_3COO^-)_2$, 1 mM EGTA, 50 mM KCH_3COO^-) and EzrA buffer 175 containing 10% glycerol with or without Thio-EzrA or Thio-EzrA(R510D). Data were collected by SpectralWorks (Olis) and exported into Microsoft Excel for data processing. Baseline corrections were applied in Excel to remove the background signal from unassembled FtsZ and the EzrA fusions.

RESULTS

Conserved seven-residue patch is required for EzrA localization to the FtsZ ring. To clarify the role of EzrA at midcell, we undertook a structure-function analysis of EzrA. Sequence alignment across 14 species predicted a conserved EzrA domain structure (Fig. 1A) consisting of an amino-terminal transmembrane anchor and a series of cytoplasmic coiled coils that vary in length and number between species. While the primary sequence conservation is generally poor, EzrA contains a well-conserved patch of 7 amino acids near its C terminus (the "QNR patch"). In *B. subtilis*, the QNR patch lies just after the fourth coiled coil, at residues 505 to 511 (IQFG NRF) (Fig. 1B).

We constructed a series of nested deletions in a functional, full-length EzrA-GFP fusion in order to identify regions essential for localization to the FtsZ ring (Fig. 1C). All *ezrA-gfp* mutant constructs were expressed from the native *ezrA* promoter and were the only copy of *ezrA* in the cell (see Materials and Methods). Full-length EzrA-GFP localizes throughout the plasma membrane and concentrates at midcell in an FtsZ-dependent manner (17). In contrast, EzrA-GFP deletions that were missing residues up to and including the fourth coiled coil (Fig. 1C) all failed to localize to midcell but were associated

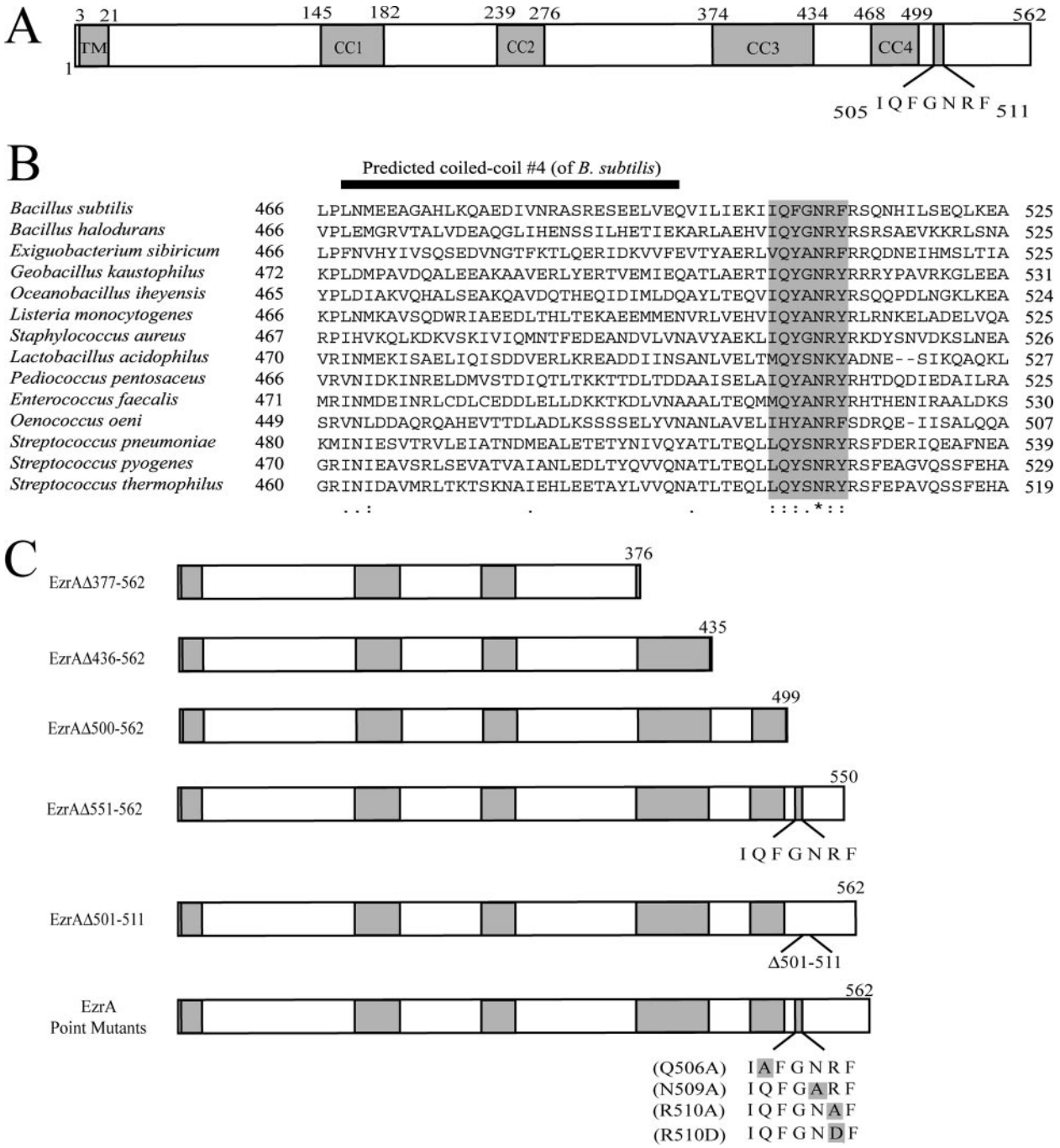

FIG. 1. EzrA contains a conserved patch of seven residues near its C terminus. (A) Predicted domain structure of *B. subtilis* EzrA, drawn to scale. The numbers indicate amino acid positions. EzrA consists of an amino-terminal transmembrane (TM) anchor, four cytoplasmic coiled-coil (CC) domains, and a C-terminal conserved-residue patch. Transmembrane and coiled-coil predictions were generated using the Simple Modular Architecture Research Tool (SMART) (http://smart.embl-heidelberg.de/). (B) Segment of EzrA alignments for low-G+C-content gram-positive bacteria, highlighting the QNR patch. The fourth predicted coiled coil of *B. subtilis* EzrA is shown for orientation but does not align precisely with the final coiled coil of other EzrAs. (C) Schematic diagram of EzrA mutants generated (with or without a GFP tag as indicated in the text) to assess EzrA localization and activity in vivo. The boxes indicate point mutations in the QNR patch.

with the plasma membrane (Fig. 2A). However, EzrAΔ551-562-GFP, a comparatively small C-terminal truncation, showed the same localization as full-length EzrA-GFP (Fig. 2A).

These results suggest that the sequence determinant for EzrA localization to the FtsZ ring lies within residues 501 to 550, a region that contains the QNR patch. In confirmation of this hypothesis, a fusion lacking the QNR patch was unable to localize to the FtsZ ring (Fig. 2B), indicating that these residues are required for medial EzrA localization.

We next employed site-directed mutagenesis to identify spe-

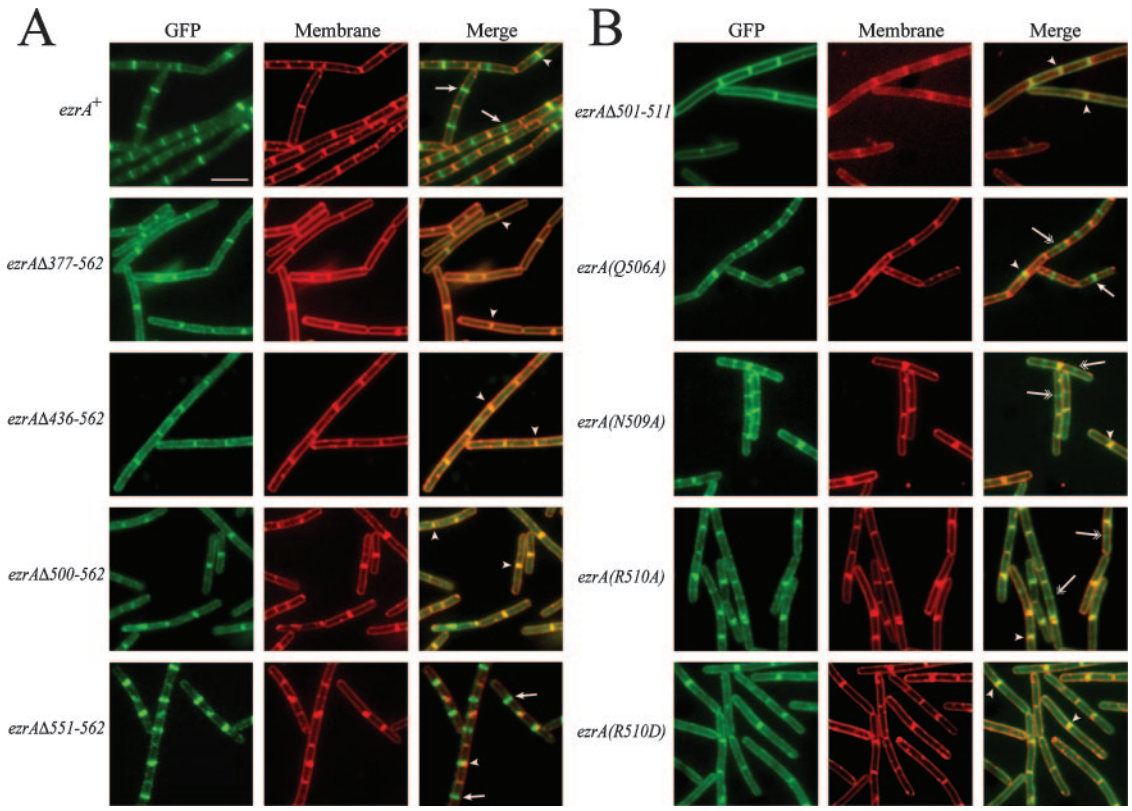

FIG. 2. The QNR patch is required for EzrA localization to the FtsZ ring. EzrA-GFP is green, and cell membranes are red. Scale bar = 5 μm. Arrows with one head indicate strong localization, arrows with two heads indicate weak localization, and arrowheads indicate EzrA localization to septa. (A) Full-length EzrA-GFP localizes to the FtsZ ring and cell membrane during exponential growth. C-terminal truncations that remove the QNR patch abolish EzrA localization to the FtsZ ring but do not affect membrane localization. (B) Removal of, or substitutions in, the QNR patch disrupt EzrA localization to the FtsZ ring.

cific residues within the QNR patch that are required for medial EzrA localization. In these experiments, we targeted the three most conserved residues for alanine substitution: Q506, N509, and R510. We also constructed an R510D charge reversal (Fig. 1C).

Fluorescence microscopy of live cells expressing various EzrA-GFP fusions indicated that single substitutions in the QNR patch disrupted EzrA localization to the FtsZ ring, albeit to different degrees (Fig. 2B and Table 2). The majority of *ezrA-gfp* cells displayed strong medial EzrA localization (Fig. 2A and Table 2). In contrast, in cells with *ezrA*(*Q506A*)*-gfp* there was a twofold decrease in the population exhibiting strong medial EzrA localization and a corresponding increase in weak localization (Fig. 2B and Table 2). This phenotype was more pronounced in *ezrA*(*N509A*)*-gfp* and *ezrA*(*R510A*)*-gfp* cells, and the majority (60 to 67%) of these cells showed no medial EzrA localization (Fig. 2B and Table 2). Notably, EzrA localization to the FtsZ ring was completely abolished in *ezrA*(*R510D*)*-gfp* cells (Fig. 2B and Table 2).

TABLE 2. EzrA localization to the FtsZ ring

Strain	% of cells (no. positive/total no.) with:		
	Strong medial localization	Weak medial localization	No medial localization
ezrA-gfp	63 (136/215)	16 (34/215)	21 (45/215)
ezrA(*Q506A*)*-gfp*	45 (123/272)	38 (102/272)	17 (47/272)
ezrA(*N509A*)*-gfp*	11 (25/227)	29 (66/227)	60 (136/227)
ezrA(*R510A*)*-gfp*	0 (0/317)	33 (105/317)	67 (212/317)
ezrA(*R510D*)*-gfp*	0 (0/136)	0 (0/136)	100 (136/136)

The loss of EzrA-GFP localization to midcell through truncations or point mutations was not due to altered EzrA or FtsZ expression. Quantitative immunoblotting indicated that the EzrA-GFP fusion proteins were the expected size, were expressed at levels comparable to the levels of full-length EzrA-GFP, and did not alter FtsZ levels (data not shown). Together, these results indicate that the QNR patch is essential for EzrA localization to the FtsZ ring.

Mutations in EzrA's QNR patch stabilize FtsZ assembly at midcell. Loss of EzrA stabilizes FtsZ assembly at midcell (17, 19), suggesting that EzrA plays an active role at this position. To test this possibility, we examined the effect of mutations in EzrA's QNR patch on the lethality associated with overexpression of the division inhibitor MinCD. During exponential growth the MinCD complex is involved in preventing inappropriate FtsZ ring formation at cell poles (20, 22); however, >12-fold overexpression of MinCD shifts the cellular balance of FtsZ dynamics towards unassembled FtsZ, blocking FtsZ ring formation and causing lethal filamentation in *B. subtilis* (20, 22). Stabilizing FtsZ assembly at midcell via a mutation in

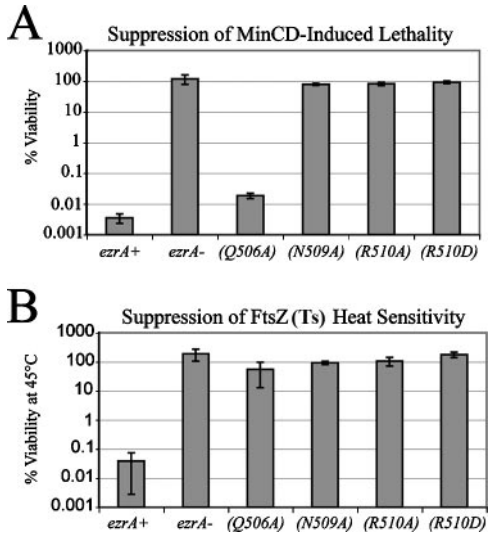

FIG. 3. Loss of medial EzrA localization stabilizes FtsZ assembly at midcell. (A) Suppression of the lethality associated with >12-fold MinCD overexpression. (B) Restoration of viability to cells with the heat-sensitive *ftsZ*(Ts) allele at the restrictive temperature (45°C). The error bars indicate standard deviations for a minimum of three replicate experiments.

a division inhibitor gene, such as *ezrA*, permits FtsZ ring formation and division even in the presence of excess MinCD (19, 29, 31).

For these experiments we cloned the four *ezrA* QNR point mutants (Fig. 1C) under control of the native *ezrA* promoter and without GFP tags into otherwise wild-type cells. Each *ezrA* QNR patch mutant was then transformed into a strain encoding an IPTG-inducible *minCD* overexpression construct, P_{spachy}-*minCD*. Viability was tested by plating cells onto medium containing 1 mM IPTG to induce >12-fold overexpression of MinCD. Removal of the GFP tag did not alter EzrA mutant stability or expression, and FtsZ levels were wild type in all strain backgrounds (data not shown).

Suppression of MinCD-induced lethality by mutations in *ezrA*'s QNR patch (Fig. 3A) correlated with the ability of individual QNR patch mutants to localize to the FtsZ ring (Fig. 2B). As expected, viability was reduced ~28,000-fold following MinCD overexpression in *ezrA*$^+$ cells (Fig. 3A). In contrast, the *ezrA* null mutant counterparts were fully viable in the presence of inducer (Fig. 3A). Of the four QNR patch mutants, those that were severely impaired in medial localization (Fig. 2B and Table 2) fully restored viability to cells in the presence of inducer. On the other hand, the *ezrA*(*Q506A*) mutation only weakly suppressed the lethality associated with MinCD overexpression (Fig. 3A), consistent with its intermediate localization phenotype (Fig. 2B and Table 2).

To extend these data, we examined the ability of the QNR patch mutants to suppress the heat sensitivity of a conditional *ftsZ* allele, *ftsZ*(Ts). At 45°C, *ftsZ*(Ts) cells fail to form FtsZ rings or septa, leading to a ~3,000-fold reduction in viability (17). Loss-of-function mutations in *ezrA* or other inhibitors of cell division restore FtsZ ring formation and viability to *ftsZ*(Ts) cells at the restrictive temperature (17, 31).

In confirmation of an active role for EzrA at midcell, loss of medial EzrA localization correlated with suppression of *ftsZ*(Ts) heat sensitivity. As expected, an *ezrA* null mutation fully restored viability to *ftsZ*(Ts) cells at the restrictive temperature (Fig. 3B). The QNR patch mutants that were most severely impaired in medial EzrA localization (Fig. 2B and Table 2) restored full viability to *ftsZ*(Ts) cells at the restrictive temperature (Fig. 3B). Conversely, EzrA(Q506A), which exhibits an intermediate medial EzrA localization phenotype (Fig. 2B and Table 2), conferred variable levels of suppression that ranged from low levels to nearly *ezrA* null mutant levels (note the relatively large error bar in Fig. 3B). These results confirm the results of the MinCD overexpression assay and are consistent with a model in which EzrA acts at midcell to destabilize FtsZ assembly at this position.

EzrA QNR patch mutants retain the ability to inhibit polar FtsZ ring formation. Aberrant, polar FtsZ ring formation is a hallmark of a loss-of-function mutation in *ezrA* (17). Polar ring formation is most likely due to an increase in FtsZ stability that overcomes MinCD activity at cell poles (19). The inability of EzrA QNR patch mutants to localize to midcell and the concurrent stabilization of the medial FtsZ ring are therefore consistent with a defect in EzrA's ability to inhibit FtsZ assembly throughout the cell. To test this possibility, we examined FtsZ ring formation in the three *ezrA* QNR patch mutants [the *ezrA*(*N509A*), *ezrA*(*R510A*), and *ezrA*(*R510D*) mutants] that showed the greatest reduction in medial EzrA-GFP localization (Fig. 2B and Table 2).

Remarkably, the three QNR patch mutants retained the ability to inhibit polar FtsZ ring formation (Fig. 4), despite the loss of medial localization (Fig. 2). Consistent with previous work, the frequency of polar FtsZ ring formation in *ezrA* null mutant cells was 15-fold higher than that in wild-type cells (Fig. 4B). Cells of two of the three QNR patch mutants [*ezrA*(*N509A*) and *ezrA*(*R510A*)] displayed FtsZ ring localization patterns that were indistinguishable from that of wild-type cells. *ezrA*(*R510D*) mutant cells exhibited a mild (3.9-fold) increase in polar ring formation (Fig. 4B). However, this increase was not statistically significant as determined by χ^2 analysis ($\alpha = 0.001$.) Together, these data indicate that the loss of localization to midcell does not eliminate EzrA's ability to inhibit FtsZ assembly at cell poles.

A purified EzrA QNR patch mutant results in inhibition of FtsZ assembly in vitro comparable to wild-type EzrA inhibition. The simplest explanation for the reduced medial localization of EzrA QNR patch mutants and the corresponding increase in FtsZ stabilization at this position would be a defect in the EzrA-FtsZ interaction. However, the ability of the QNR patch mutants to inhibit polar FtsZ ring formation suggests that the EzrA-FtsZ interaction is at least partially intact. To resolve this issue, we examined the ability of the EzrA(R510D) mutant to inhibit FtsZ assembly in vitro. We chose this mutant as it exhibited the greatest reduction in medial localization (Fig. 2B and Table 2). For purification purposes we constructed a six-His-tagged version of EzrA(R510D), substituting a thioredoxin moiety for its N-terminal transmembrane anchor [Thio-EzrA(R510D)]. The relative levels of FtsZ assembly were measured in real time by 90°-angle light scattering (23) in the presence or absence of wild-type Thio-EzrA or Thio-EzrA(R510D).

Consistent with previous results (8), addition of 1 mM GTP

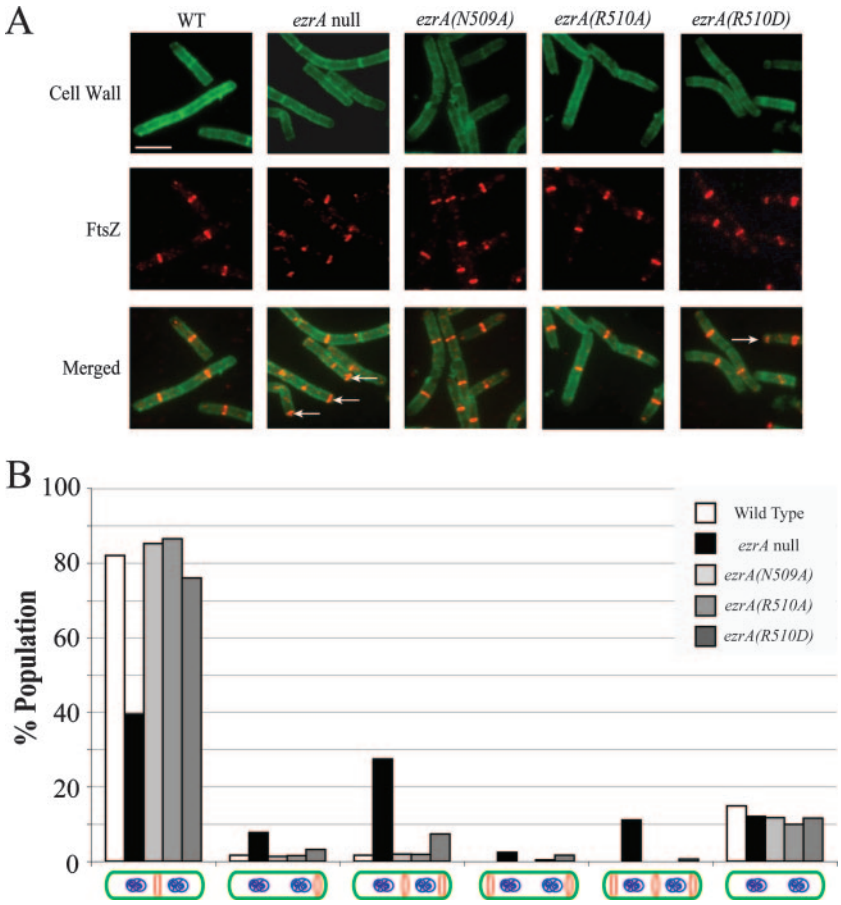

FIG. 4. Disruption of EzrA medial localization does not interfere significantly with the ability of EzrA to inhibit polar FtsZ ring formation. (A) Immunofluorescence microscopy of fixed cells stained for FtsZ (red) and cell wall (green). Scale bar = 5 μm. The arrows indicate polar FtsZ rings. (B) FtsZ localization patterns in wild-type, *ezrA* null mutant, *ezrA*(*N509A*) mutant, *ezrA*(*R510A*) mutant, and *ezrA*(*R510D*) mutant cells.

to a reaction mixture containing 5 μM purified FtsZ led to a rapid increase in light scattering, while the presence of 10 μM purified Thio-EzrA decreased FtsZ light scattering by ~60% (Fig. 5A). This result was typical for wild-type EzrA purified using the two-step protocol described in Materials and Methods. Strikingly, Thio-EzrA(R510D) inhibited FtsZ assembly to the same degree as its wild-type counterpart (Fig. 5A), even at low concentrations (Fig. 5B). These data indicate that Thio-EzrA(R510D) is wild type with regard to its ability to interact with FtsZ in vitro and are consistent with data indicating that QNR patch mutants interact with FtsZ in vivo to inhibit polar FtsZ ring formation (Fig. 4).

Loss of medial EzrA localization leads to an increase in cell length that is independent of polar ring formation. Cells lacking *ezrA* are longer than wild-type cells (4, 14, 17). It has been suggested that the increased size of *ezrA* null mutant cells results from dilution of division components at midcell due to the presence of extra FtsZ rings at cell poles (14). Alternatively, changes in FtsZ polymer dynamics in the absence of EzrA activity at midcell may be responsible for increases in cell size. In support of the latter model, *ezrA* null mutant cells are longer than wild-type cells even under conditions that do not support the formation of extra FtsZ rings (i.e., growth in minimal glucose medium) (17).

To determine whether the loss of EzrA activity at midcell is the proximal cause of the increase in cell length observed in *ezrA* null mutants, we measured the lengths of QNR patch mutant cells in both nutrient-rich (LB) and nutrient-poor ($S7_{50}$-minimal glucose [13]) media. If EzrA plays an active role at midcell, then *ezrA* QNR patch mutant cells should be longer than wild-type cells despite the low frequency of polar ring formation. Conversely, if the increased length of *ezrA* null mutant cells is a consequence of extra FtsZ ring formation at cell poles, then *ezrA* QNR patch mutants should exhibit a wild-type cell length distribution.

Our data indicate that EzrA localization to midcell is essential for maintaining proper cell size, regardless of polar FtsZ ring formation. Wild-type cells cultured in LB medium had a mean length of ~4.0 μm, while *ezrA* null mutant cells were ~75% longer (mean length, ~7.0 μm). For the QNR patch mutants, cell length (Fig. 6) correlated with localization pattern (Fig. 2 and Table 2). The cells of the two mutants that displayed an intermediate EzrA localization phenotype [the *ezrA*(*N509A*) and *ezrA*(*R510A*) mutants] had average lengths that were ~23% greater (mean length, ~4.9 μm) than the length of wild-type cells. *ezrA*(*R510D*) mutant cells, which are completely defective in medial EzrA localization, were ~45% longer than wild-type cells (mean length, ~5.8 μm). Together,

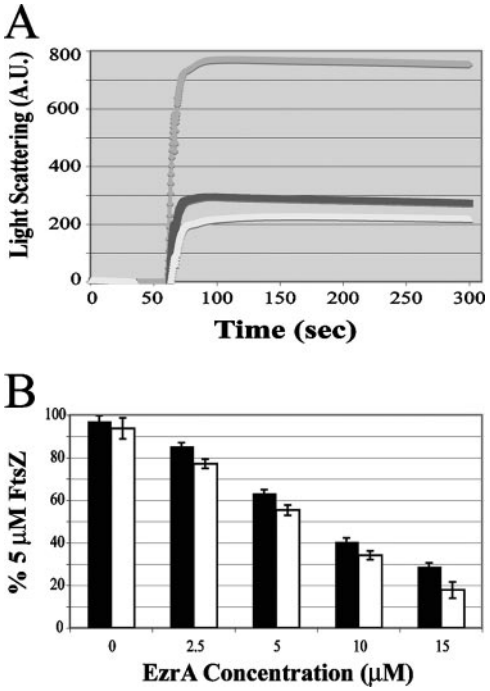

FIG. 5. Inhibition of FtsZ assembly in vitro by purified Thio-EzrA(R510D) is comparable to the inhibition by wild-type Thio-EzrA. (A) Representative traces of FtsZ assembly from 90°-angle light-scattering assays. Gray trace, FtsZ plus GTP; black trace, FtsZ plus Thio-EzrA plus GTP; white trace, FtsZ plus Thio-EzrA(R510D) plus GTP. The concentration of FtsZ was 5 μM, the concentration of EzrAs was 10 μM, and the concentration of GTP was 1 mM. A.U., arbitrary units. (B) Inhibition of 5 μM FtsZ assembly by Thio-EzrA(R510D) (open bars) is comparable to the inhibition by wild-type Thio-EzrA (filled bars) across a range of concentrations. The error bars indicate standard deviations for five replicate experiments.

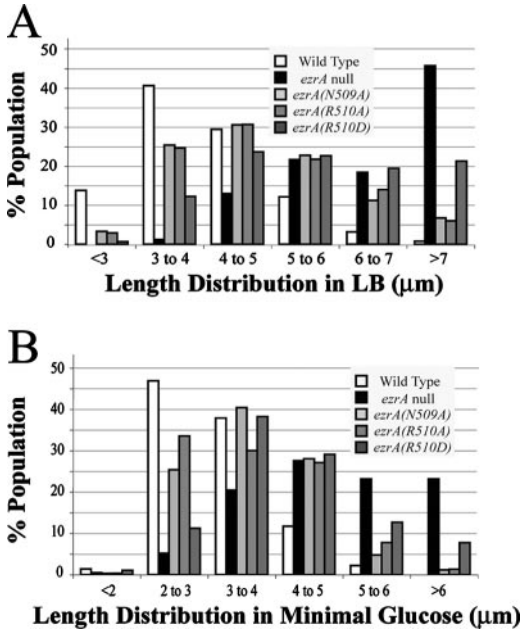

FIG. 6. Loss of medial EzrA localization leads to an increase in cell length that is independent of polar ring formation. Cell length distribution was determined for strains grown in (A) LB and (B) minimal glucose media.

these data show that there was a significant shift in cell length distribution upon disruption of medial EzrA localization (Fig. 6A), even when few polar rings were present.

We next examined the lengths of wild-type and *ezrA* mutant cells cultured in $S7_{50}$-minimal glucose medium. These growth conditions do not support the formation of extra FtsZ rings, although *ezrA* null mutant populations contain a low percentage of cells with single polar FtsZ rings (17). As expected, wild-type *B. subtilis* cells cultured in minimal medium were substantially shorter than their counterparts cultured in LB medium (27), with an average length of ~3.2 μm. Although shorter than cells cultured in LB medium, *ezrA* null cells cultured under these conditions were still ~59% longer than wild-type cells (mean length, ~5.0 μm). Like mutants cultured in LB medium, *ezrA* QNR patch mutants grown in minimal medium also showed a statistically significant increase in cell length compared to the wild-type strain. Cells of the *ezrA*(*N509A*) and *ezrA*(*R510A*) mutants were both ~6% longer than wild-type cells (mean length, ~3.6 μm), and cells of the more severe *ezrA*(*R510D*) mutant were ~31% longer (mean length, ~4.2 μm). The intermediate length of the *ezrA*(*R510D*) mutant cells in LB and minimal glucose media (Fig. 6) suggests that this mutant retained some residual activity at midcell, despite showing no medial EzrA localization by fluorescence microscopy (Fig. 2). The frequency of minicell formation in *ezrA* null mutants and *ezrA* QNR patch mutants was less than 4% in both minimal glucose and LB media (data not shown); thus, polar septation events that occur at the expense of binary fission are unlikely to be the explanation for increases in cell length.

As further evidence of a disturbance in cell size homeostasis, the *ezrA* QNR patch mutants exhibited an increase in the ratio of cell length to FtsZ rings (L/R ratio). Wild-type cells exhibited an L/R ratio of ~6.5 μm/ring under a range of growth conditions (29). Conversely, the L/R ratio of *ezrA* null mutant cells increased by ~31% (~8.5 μm/ring) after growth in LB medium, despite the presence of extra FtsZ rings. Two of the QNR patch mutants, the *ezrA*(*N509A*) and *ezrA*(*R510A*) mutants, each had a ~7% increase in the L/R ratio (~6.9 μm/ring), and the *ezrA*(*R510D*) mutant had a ~19% increase in the L/R ratio (~7.7 μm/ring). The widths of wild-type and *ezrA* mutant cells were statistically indistinguishable (data not shown).

Importantly, the percentage of *ezrA* mutant cells that contained FtsZ rings was identical to the percentage of wild-type cells that contained FtsZ rings (Fig. 4), and the mass doubling times were also identical (data not shown). These data indicate that the timing of FtsZ ring formation relative to cell birth and the duration of the Z-period were not perturbed. If loss of medial EzrA activity affected either of these two parameters, we would have expected to see changes in FtsZ ring frequency in an *ezrA* null mutant cell population compared to the wild-type cell population. This is counter to previous reports suggesting that FtsZ ring constriction is delayed in *ezrA* null mutants during slow growth (14). The difference between our results and those of Kawai and Ogasawara (14) may reflect differences in strain background, media, and/or temperature

(e.g., our measurements were obtained with cells cultured in liquid medium at 37°C, whereas Kawai and Ogasawara used slow-growing cells cultured on solid medium at 24°C [14]). Together, these data indicate that the increased length of *ezrA* mutant cells is due to loss of EzrA activity at midcell rather than to dilution of division components in the presence of extra FtsZ rings at cell poles.

DISCUSSION

We identified a conserved seven-residue patch (the QNR patch) in the C terminus of EzrA (Fig. 1A and B) that is required for interaction with the preformed FtsZ ring. A single substitution in the QNR patch abolishes medial EzrA localization (Fig. 2) but does not alter the ability of EzrA to inhibit FtsZ assembly in vitro (Fig. 5) and results in only a modest increase in polar FtsZ ring formation (Fig. 4).

The isolation of *ezrA* mutants that are specifically defective for medial localization allowed us to clarify the role of EzrA at the cytokinetic ring. Notably, our data indicate that EzrA contributes to FtsZ assembly dynamics within the medial ring, thereby helping to coordinate division with cell growth and ensuring that cells are the proper length upon cytokinesis. QNR patch mutants were resistant to overexpression of the MinCD division inhibitor (Fig. 3) and exhibited increases in cell length (Fig. 6), consistent with stabilization of FtsZ assembly at midcell. The increases in cell length were unlikely to be due to a reduction in the cytoplasmic pool of division components, as *ezrA* QNR patch mutant cells exhibited a pattern of FtsZ ring formation that was statistically indistinguishable from that of wild-type cells. Moreover, we saw a similar increase in *ezrA* null mutant cell length in minimal medium (Fig. 6), conditions that do not support the formation of extra FtsZ rings (17). It is possible that *ezrA* QNR patch mutants possess a higher percentage of large FtsZ polymers even in the absence of extra FtsZ rings, a situation that might effectively sequester components of the division apparatus away from midcell. However, this explanation seems unlikely given the significant stabilization of FtsZ assembly at midcell in the *ezrA* QNR patch mutant backgrounds.

The idea that EzrA destabilizes FtsZ assembly at midcell appears to conflict with FRAP data indicating that FtsZ turnover rates are identical in wild-type and *ezrA* null mutant cells (1). However, FRAP also shows that the half-life of an FtsZ subunit in the cytokinetic ring varies significantly from 4 to 20 s, even in wild-type cells (1). Thus, it is possible that the loss of *ezrA* has a modest effect on subunit turnover that is undetectable by FRAP, yet sufficient to alter the stability of the medial FtsZ ring. Alternatively, the loss of EzrA may stabilize the FtsZ ring in a manner that does not significantly decrease subunit turnover itself (e.g., boosting nucleation potential at midcell or increasing the number of polymers in the ring itself).

Our data indicating that the frequency of FtsZ ring formation and the duration of the Z-period are not perturbed in *ezrA* mutant cells (Fig. 4) argue against a model in which the increase in cell length is due to changes in the timing of cytokinesis and/or in the persistence of the FtsZ ring, as previously suggested (14). Instead, we favor a model in which the loss of EzrA activity at midcell increases the stability of the medial FtsZ ring, rendering it resistant to the factors responsible for coordinating division with cell size. This situation would be analogous to the increase in FtsZ polymer stability that overcomes the activity of the MinCD complex at the poles of *ezrA* null mutant cells (19).

Despite being defective in medial localization (Fig. 2), EzrA QNR patch mutants are similar to wild-type EzrA with regard to the ability to inhibit aberrant FtsZ assembly at cell poles (Fig. 4). The data indicate that QNR patch mutants have not lost the ability to interact with FtsZ, consistent with our in vitro data (Fig. 5). It remains formally possible that in the absence of medial EzrA localization there is an increase in EzrA concentrations at the cell poles that compensates for a decreased EzrA-FtsZ interaction, thus allowing inhibition of polar FtsZ assembly to persist. However, EzrA(R510D), which is completely defective in medial localization, inhibits FtsZ assembly in vitro to wild-type levels (Fig. 5), suggesting that the EzrA-FtsZ interaction remains robust.

Based on these results, we propose that EzrA has at least two separate regions for interaction with FtsZ. The first region, located in the N-terminal portion of EzrA, is required for the interaction between EzrA and the free FtsZ monomers and multimers that constitute the cytoplasmic pool of FtsZ. The second region, contained in the QNR patch, promotes interaction with the single-stranded polymers and bundles that constitute the FtsZ ring but is dispensable for inhibition of de novo FtsZ assembly. Alternatively, the QNR patch may be required for interaction between EzrA and another component of the cytokinetic ring, thereby bringing EzrA into close proximity with FtsZ at this position. A fusion of the QNR patch to the C terminus of GFP was unable to localize to the FtsZ ring on its own, indicating that, while necessary, this fusion is not sufficient for medial localization (D. P. Haeusser, unpublished data).

Together, our results support a model in which EzrA has two distinct functions in vivo: one in which it prevents aberrant FtsZ assembly at cell poles, as previously characterized (8, 17, 19), and one in which it destabilizes FtsZ assembly at midcell, enhancing the dynamic nature of the medial FtsZ ring and ensuring that division is coupled to cell growth. Future work will address whether the QNR patch of EzrA is required for interaction with preformed FtsZ polymers or for interaction with other division proteins. Our results highlight the need for a more comprehensive understanding of the molecular nature of the FtsZ interaction with its modulating proteins, particularly those that appear to interact with FtsZ at more than one subcellular location.

ACKNOWLEDGMENTS

We thank P. Chivers, H. Erickson, and D. Rudner for the generous gift of plasmids or strains and D. Gregg, N. Hill, R. Kranz, M. Oates-Leslie, Q. Luo, L. Romberg, and R. Weart for technical assistance, advice, and/or insightful comments on the manuscript. We are also grateful to members of the Levin laboratory for useful discussions during the course of this research.

This work was supported in part by Public Health Service grant GM64671 from the NIH and by National Science Foundation CAREER award MCB-0448186 to P.A.L. A.Z.B. was funded in part by a Ruth L. Kirschstein National Research Service Award from the NIH (grant F32-GM077828). A.C.G. was funded in part by a summer undergraduate research fellowship from the Howard Hughes Medical Institute.

REFERENCES

1. **Anderson, D. E., F. J. Gueiros-Filho, and H. P. Erickson.** 2004. Assembly dynamics of FtsZ rings in *Bacillus subtilis* and *Escherichia coli* and effects of FtsZ-regulating proteins. J. Bacteriol. **186:**5775–5781.
2. **Benson, A. K., and W. G. Haldenwang.** 1993. Regulation of σ^B levels and activity in *Bacillus subtilis*. J. Bacteriol. **175:**2347–2356.
3. **Chivers, P. T., and R. T. Sauer.** 1999. NikR is a ribbon-helix-helix DNA-binding protein. Protein Sci. **8:**2494–2500.
4. **Chung, K. M., H. H. Hsu, S. Govindan, and B. Y. Chang.** 2004. Transcription regulation of *ezrA* and its effect on cell division of *Bacillus subtilis*. J. Bacteriol. **186:**5926–5932.
5. **Chung, K. M., H. H. Hsu, H. Y. Yeh, and B. Y. Chang.** 2007. Mechanism of regulation of prokaryotic tubulin-like GTPase FtsZ by membrane protein EzrA. J. Biol. Chem. **282:**14891–14897.
6. **Errington, J., R. A. Daniel, and D. J. Scheffers.** 2003. Cytokinesis in bacteria. Microbiol. Mol. Biol. Rev. **67:**52–65.
7. **Guzman, L. M., D. Belin, M. J. Carson, and J. Beckwith.** 1995. Tight regulation, modulation, and high-level expression by vectors containing the arabinose P_{BAD} promoter. J. Bacteriol. **177:**4121–4130.
8. **Haeusser, D. P., R. L. Schwartz, A. M. Smith, M. E. Oates, and P. A. Levin.** 2004. EzrA prevents aberrant cell division by modulating assembly of the cytoskeletal protein FtsZ. Mol. Microbiol. **52:**801–814.
9. **Hale, C. A., and P. A. J. de Boer.** 1997. Direct binding of FtsZ to ZipA, an essential component of the septal ring structure that mediates cell division in *E. coli*. Cell **88:**175–185.
10. **Harry, E., L. Monahan, and L. Thompson.** 2006. Bacterial cell division: the mechanism and its precision. Int. Rev. Cytol. **253:**27–94.
11. **Harwood, C. R., and S. M. Cutting (ed.).** 1990. Molecular biological methods for *Bacillus*. John Wiley and Sons, Chichester, United Kingdom.
12. **Ireton, K., D. Z. Rudner, K. J. Siranosian, and A. D. Grossman.** 1993. Integration of multiple developmental signals in *Bacillus subtilis* through the Spo0A transcription factor. Genes Dev. **7:**283–294.
13. **Jaacks, K. J., J. Healy, R. Losick, and A. D. Grossman.** 1989. Identification and characterization of genes controlled by the sporulation-regulatory gene *spo0H* in *Bacillus subtilis*. J. Bacteriol. **171:**4121–4129.
14. **Kawai, Y., and N. Ogasawara.** 2006. *Bacillus subtilis* EzrA and FtsL synergistically regulate FtsZ ring dynamics during cell division. Microbiology **152:**1129–1141.
15. **Lemon, K. P., I. Kurtser, and A. D. Grossman.** 2001. Effects of replication termination mutants on chromosome partitioning in *Bacillus subtilis*. Proc. Natl. Acad. Sci. USA **98:**212–217.
16. **Levin, P. A.** 2002. Light microscopy techniques for bacterial cell biology, p. 115–132. *In* P. J. Sansonetti and A. Zychlinsky (ed.), Molecular cellular microbiology. Academic Press, Ltd., London, United Kingdom.
17. **Levin, P. A., I. G. Kurtser, and A. D. Grossman.** 1999. Identification and characterization of a negative regulator of FtsZ ring formation in *Bacillus subtilis*. Proc. Natl. Acad. Sci. USA **96:**9642–9647.
18. **Levin, P. A., and R. Losick.** 1996. Transcription factor Spo0A switches the localization of the cell division protein FtsZ from a medial to a bipolar pattern in *Bacillus subtilis*. Genes Dev. **10:**478–488.
19. **Levin, P. A., R. L. Schwartz, and A. D. Grossman.** 2001. Polymer stability plays an important role in the positional regulation of FtsZ. J. Bacteriol. **183:**5449–5452.
20. **Levin, P. A., J. J. Shim, and A. D. Grossman.** 1998. Effect of *minCD* on FtsZ ring position and polar septation in *Bacillus subtilis*. J. Bacteriol. **180:**6048–6051.
21. **Margolin, W.** 2005. FtsZ and the division of prokaryotic cells and organelles. Nat. Rev. Mol. Cell Biol. **6:**862–871.
22. **Marston, A. L., and J. Errington.** 1999. Selection of the midcell division site in *Bacillus subtilis* through MinD-dependent polar localization and activation of MinC. Mol. Microbiol. **33:**84–96.
23. **Mukherjee, A., and J. Lutkenhaus.** 1999. Analysis of FtsZ assembly by light scattering and determination of the role of divalent metal cations. J. Bacteriol. **181:**823–832.
24. **Perego, M., G. B. Spiegelman, and J. A. Hoch.** 1988. Structure of the gene for the transition state regulator *abrB*: regulator synthesis is controlled by the *spo0A* sporulation gene in *Bacillus subtilis*. Mol. Microbiol. **2:**689–699.
25. **Romberg, L., and P. A. Levin.** 2003. Assembly dynamics of the bacterial cell division protein FtsZ: poised at the edge of stability. Annu. Rev. Microbiol. **57:**125–154.
26. **Sambrook, J., E. F. Fritsch, and T. Maniatis.** 1989. Molecular cloning: a laboratory manual, 2nd ed. Cold Spring Harbor Laboratory Press, Cold Spring Harbor, NY.
27. **Sargent, M. G.** 1975. Control of cell length in *Bacillus subtilis*. J. Bacteriol. **123:**7–19.
28. **Singh, J. K., R. D. Makde, V. Kumar, and D. Panda.** 24 August 2007, posting date. A membrane protein, EzrA, regulates assembly dynamics of FtsZ by interacting with the C-terminal tail of FtsZ. Biochemistry. doi:10.1021/bi700710j.
29. **Weart, R. B., A. H. Lee, A. C. Chien, D. P. Haeusser, N. S. Hill, and P. A. Levin.** 2007. A metabolic sensor governing cell size in bacteria. Cell **130:**335–347.
30. **Weart, R. B., and P. A. Levin.** 2003. Growth rate-dependent regulation of medial FtsZ ring formation. J. Bacteriol. **185:**2826–2834.
31. **Weart, R. B., S. Nakano, B. E. Lane, P. Zuber, and P. A. Levin.** 2005. The ClpX chaperone modulates assembly of the tubulin-like protein FtsZ. Mol. Microbiol. **57:**238–249.
32. **Wu, L. J., and J. Errington.** 2004. Coordination of cell division and chromosome segregation by a nucleoid occlusion protein in *Bacillus subtilis*. Cell **117:**915–925.